

Attributing increases in fire weather to anthropogenic climate change over France

Renaud Barbero^{1,*}, John T. Abatzoglou^{2,3}, François Pimont⁴, Julien Ruffault⁴, Thomas Curt¹

¹INRAE, Ecosystèmes Méditerranéens et Risques, Aix-en-Provence, France

²Department of Geography, University of Idaho, Moscow, United States

³Management of Complex Systems Department, University of California, Merced, California, United States

⁴INRAE, Ecologie des Forêts Méditerranéennes, Avignon, France

Correspondence*:
Corresponding Author
renaud.barbero@inrae.fr

1 SUPPLEMENTARY INFORMATION

- 2 Sherwood, S. C., Bony, S., Dufresne, J. L. (2014). Spread in model climate sensitivity traced to atmospheric
3 convective mixing. *Nature*. <https://doi.org/10.1038/nature12829>

Name	lat × lon	huss	ECS
BCC-CSM1-1	2.7905 × 2.8125	x	2.88
CANESM2	2.7905 × 2.8125		3.68
CNRM-CM5	1.4008 × 1.4063	x	3.25
CSIRO-MK3-6-0	1.8652 × 1.875		3.99
GFDL-CM3	2 × 2.5		3.96
GFDL-ESM2G	2.0225 × 2.5		2.38
GFDL-ESM2M	2.0225 × 2.5		2.41
HADGEM2-CC	1.25 × 1.875	x	-
HADGEM2-ES	1.25 × 1.875		4.55
INMCM4	1.5 × 2	x	2.07
IPSL-CM5A-LR	1.8947 × 3.75	x	4.10
IPSL-CM5A-MR	1.2676 × 2.5	x	-
IPSL-CM5B-LR	1.8947 × 3.75	x	2.59
MIROC-ESM-CHEM	2.7905 × 2.8125	x	-
MIROC-ESM	2.7905 × 2.8125	x	4.65
MIROC5	1.4008 × 1.4063		2.71
MRI-CGCM3	1.1215 × 1.125	x	2.59

Table 1. List of the 17 climate models from the Coupled Model Intercomparison Project, Phase 5 (CMIP5) used in the study. The first ensemble member (r1i1p1) was used for each model. Models where rhsmin was not archived prior to 1950 are denoted in the third column. A bias correction procedure was used for these models to estimate rhsmin prior to the archival in historical runs. The fourth column shows the equilibrium climate sensitivity (ECS) as reported by Sherwood et al. (2014).

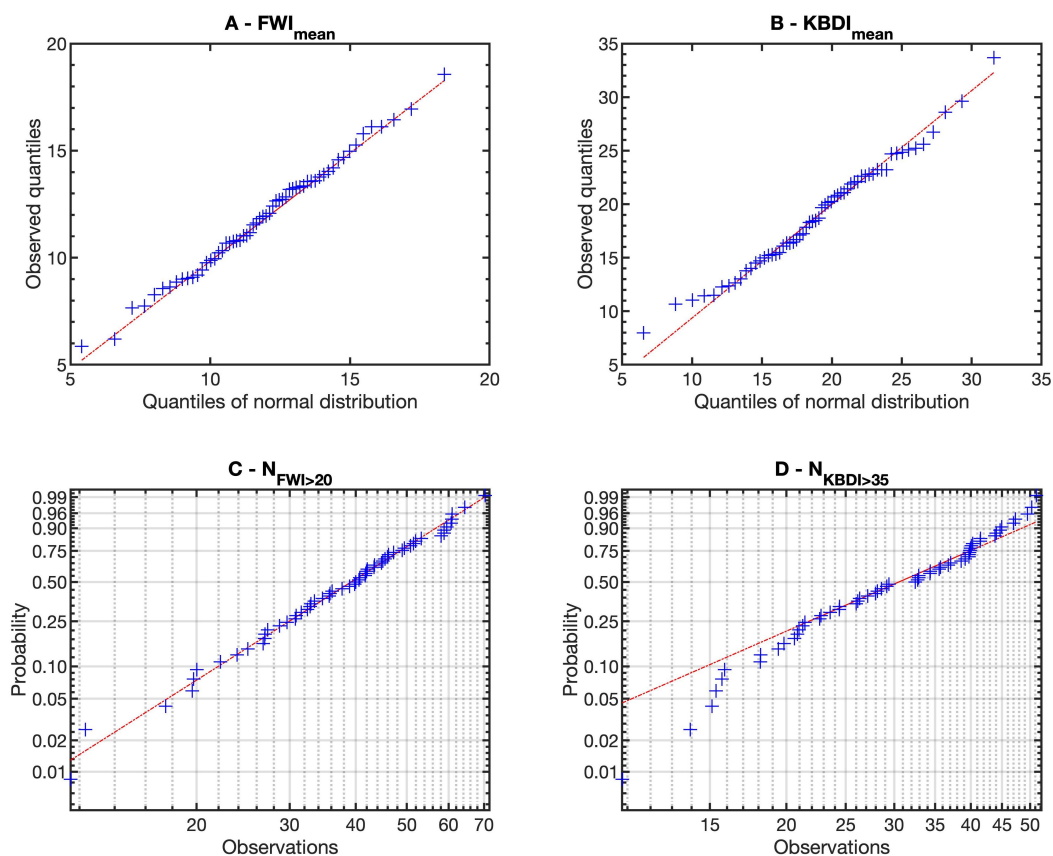


Figure S1. a) Quantile-quantile plot of the quantiles of the mean observed FWI from May-September averaged across the Mediterranean region versus the theoretical quantile values from a normal distribution. The red line indicates the theoretical distribution. b) Same as a) but for KBDI. c) Weibull probability plot for the annual number of occurrence of daily FWI > 20 averaged across the Mediterranean region. d) Same as c) but for the annual number of occurrence of daily KBDI > 35.

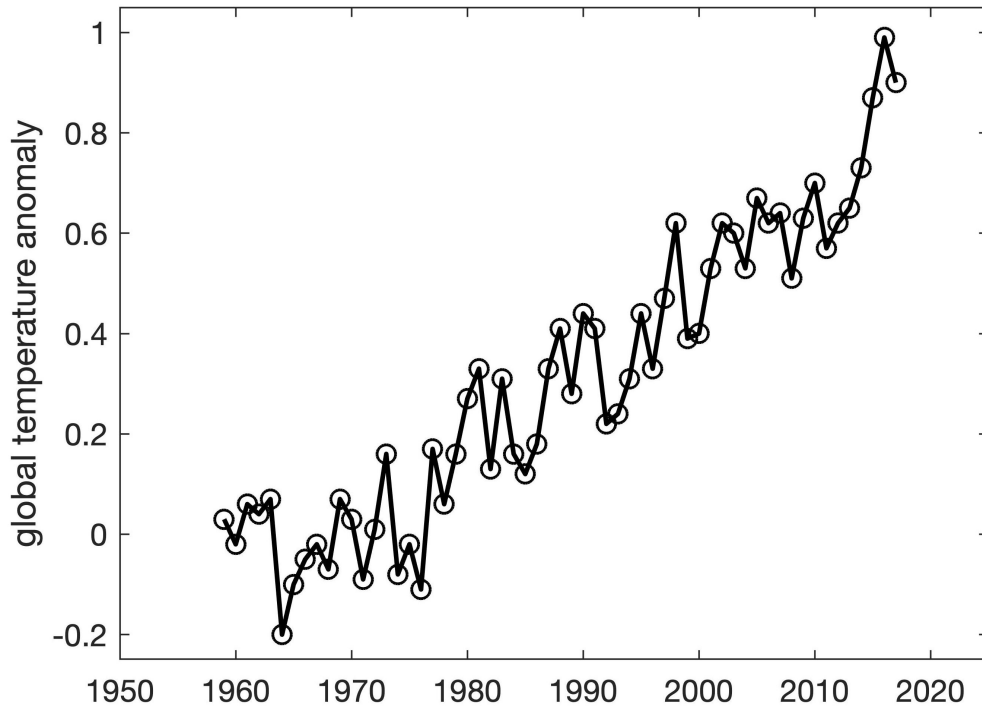


Figure S2. Global mean surface temperature anomaly series where anomalies have been calculated with respect to the 1951–80 baseline period.

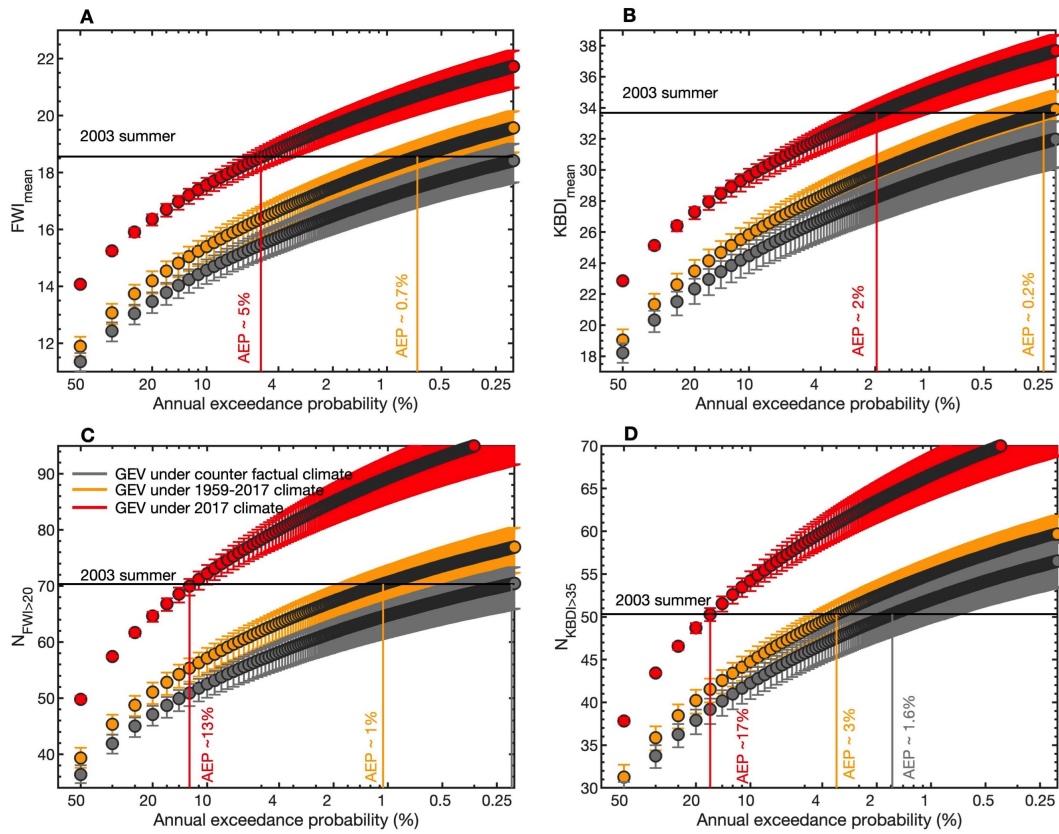


Figure S3. Same as figure 4 but with the global mean surface temperature anomaly (see Figure S3) as a covariate in the non-stationary fit.

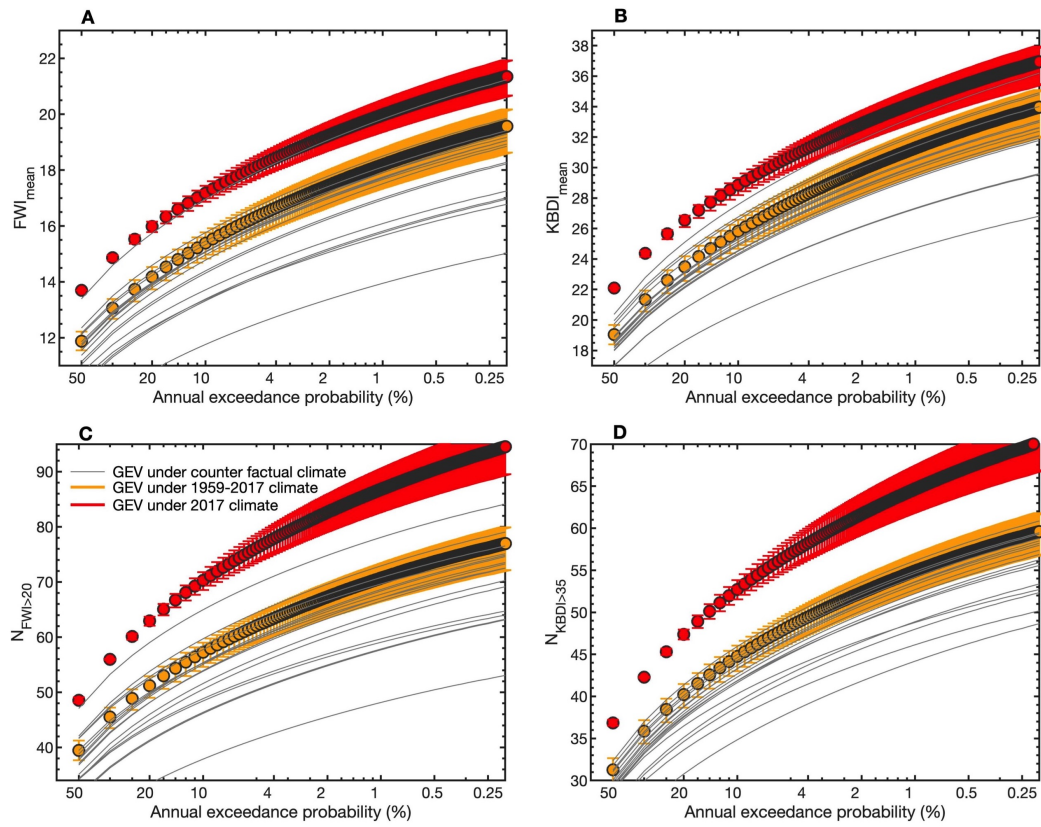


Figure S4. Same as figure 4 but for individual counterfactual observations (gray). Note that only the best estimates for each counterfactual observations are shown for clarity.